Ferromagnetic Mn(II)···Cu(II) Exchange in the New Bimetallic Quasi-2-D Compound $Cu(op)_2MnCl_4$ (op = 1,4-Diazacycloheptane)

B. Chiari,[†] A. Cinti,[†] L. David,[§] F. Ferraro,[§] D. Gatteschi,[§] O. Piovesana,*[,†] and P. F. Zanazzi[‡]

Dipartmento di Chimica and Dipartimento di Scienza della Terra, Sezione Cristallografia, Università di Perugia, 06100 Perugia, Italy, and Dipartimento di Chimica, Università di Firenze, Florence, Italy

Received April 4, 1996[⊗]

The synthesis, crystal structure, and magnetic properties are reported for the new bimetallic compound $Cu(op)_2MnCl_4$, where op = $HN(CH_2)_5NH$. The compound, $C_{10}H_{24}N_4Cl_4CuMn$, crystallizes in the monoclinic space group $P2_1/n$. Cell dimensions are as follows: $a = 15.316(3)$ Å, $b = 16.608(3)$ Å, $c = 7.141(2)$ Å, $\beta = 100.01(5)°$, $Z = 4$. The structure consists of well-separated and magnetically equivalent layers which are composed of chloride-bridged $Cu(op)_2MnCl_4$ binuclear units connected by rather loose Cu−N−H···Cl−Mn contacts. The $MnCl_4$ fragment approximates tetrahedral symmetry. The Cu(II) geometry is (4 + 1) square-pyramidal with the apical position occupied by a bridging chloride ligand and the basal ones by the nitrogen atoms from the organic ligands. The shortest interlayer M···M separations, ∼7 Å, are of the Mn···Cu type. Magnetic susceptibility and single-crystal EPR measurements for the compound have been carried out over the range 4−300 K. At room temperature the χT product (per MnCu unit) has a value of 4.84 emu·mol^{-1}·K, close to that expected for uncoupled $S = {}^5/_2$ and $S = {}^1/_2$ spins. When the temperature is lowered, χT remains almost constant until 80−90 K, slightly increases to reach a maximum at ∼13 K (5.21 emu·mol^{-1}·K), and then rapidly decreases. Comparison between theory and experiment, made with use of both a mean field corrected dimer model and an approximate 2-D model, indicates that Mn(II)···Cu(II) exchange is ferromagnetic within the dimers ($J_1 \sim 2.6$ cm^{-1}) and antiferromagnetic among dimers, with J values between −0.07 and −0.03 cm^{-1} (the interaction Hamiltonian is of the form $H = -2J\mathbf{S}_A\cdot\mathbf{S}_B$). Single-crystal EPR spectra recorded along the *a*, *b*, and *c** axes show a large temperature dependence of the *g* factors: at 4.2 K, $g_a = 2.10$, $g_b = 1.96$, and $g_{c^*} = 2.01$. This pattern substantiates the presence of a 2-D magnetic structure with ferromagnetic intradimer exchange and interdimer antiferromagnetic exchange of weaker magnitude. The opposite signs of the interactions are ascribed to the local symmetries of the Cu(II) and Mn(II) ions.

Introduction

Ordinarily one expects the sign of an exchange-coupling constant to be crucially dependent on the geometry of the system.[1] For Cu(II) dimers and chains, for instance, there is considerable experimental evidence for the continuum in exchange coupling from positive to negative exchange-coupling constants.[2]

Conversely, on the basis of orbital arguments initially proposed by Anderson and others,[3] Kahn and co-workers[4] have suggested that an intrinsic antiferromagnetic interaction is to be expected for a Mn(II)($S={}^5/_2$)−Cu(II)($S={}^1/_2$) pair, irrespective of local symmetries. Indeed, the factors leading to the existence of ferromagnetic coupling for such a pair remain an open question.[5]

The Kahn concept has encouraged an intensive and successful search for bimetallic compounds of Mn(II) and Cu(II) behaving as bulk ferromagnets. The subject has been reviewed extensively.[6−8]

Basically, provided that Mn(II) and Cu(II) are antiferromagnetically coupled on all occasions, the requirement for such materials is an ordered alternation of the Mn(II) and Cu(II) ions throughout the crystal lattice. If so, below some transition temperature the intrinsic antiferromagnetic nn interactions tend to align the S_{Mn} and S_{Cu} sublattices antiparallel and the material retains a net magnetic moment because the two sublattices are not equivalent.

Some of us have recently described two systems, namely, $Cu(en)_2MnCl_4$ (en = ethylenediamine)[5] and $\{[Cu(en)_2]_3[Mn(NCS)_6]\}(NCS)_2$,[9] which do not conform to the above expectation. In particular, the former compound, in spite of a structure in which cross-linked −Cu−Cl−Mn−Cl−Cu− and −Cu−N−H···Cl−Mn− chains form well-isolated layers and where the shortest interlayer M···M contacts are of the Mn···-

[†] Dipartimento di Chimica, Universitá di Perugia.
[‡] Dipartimento di Scienza della Terra, Universitá di Perugia.
[§] Università di Firenze.
* To whom correspondence should be addressed at the Dipartimento di Chimica.

[⊗] Abstract published in *Advance ACS Abstracts,* November 15, 1996.

(1) See various articles in: *Magneto-Structural Correlations in Exchange-Coupled Systems*; Reidel: Dordrecht, The Netherlands, 1985.
(2) Hatfield, W. E. *Inorg. Chem.* **1983**, *22*, 833, and references cited therein.
(3) Ginsberg, A. *Inorg. Chim. Acta Rev.* **1971**, *5*, 45, and references cited therein.
(4) Kahn, O. *Struct. Bonding (Berlin)* **1987**, *68*, 89, and references cited therein.
(5) Chiari, B.; Cinti, A.; Piovesana, O.; Zanazzi, P. F. *Inorg. Chem.* **1995**, *34*, 2652.
(6) *Proceedings of the Fourth International Conference on Molecule-Based Magnets*; Miller, J. S.; Epstein A. J., Eds.; Molecular Crystals and Liquid Crystals; Gordon & Breach: London, 1995. *Proceedings of the International Symposium on Chemistry and Physics of Molecular Based Magnetic Materials*; Iwamura, H., Itoh, K., Kinoshita, M., Eds.; Molecular Crystals and Liquid Crystals; Gordon & Breach: London, 1993.
(7) See various articles in *Magnetic Molecular Materials*; Gatteschi, D., Kahn, O., Miller, J. S., Palacio, F., Eds; NATO ASI Series; Kluwer: Dordrecht, The Netherlands, 1991.
(8) Stumpf, H. O.; Pei, Y.; Kahn, O.; Sletten, J.; Renard, J. P. *J. Am. Chem. Soc.* **1993**, *115*, 6738, and references cited therein.
(9) Burla, M. C.; Chiari, B.; Cinti, A.; Piovesana, O. *Mol. Cryst. Liq. Cryst.* **1995**, *273*, 211.

S0020-1669(96)00373-4 CCC: $12.00

Table 1. Crystallographic Data for $Cu(op)_2MnCl_4$

formula	$C_{10}H_{24}N_4Cl_4CuMn$	Z	4
fw	460.7	T, °C	20
space group	$P2_1/n$	λ, Å	0.7107
a, Å	15.316(3)	ρ, g·cm^{-3}	1.711
b, Å	16.608(3)	μ, cm^{-1}	24.7
c, Å	7.141(2)	R^a	0.059
β, deg	101.01(5)	$R_w{}^b$	0.062
V, Å^3	1788.8		

[a] $R = \sum(|F_o| - |F_c|)/\sum|F_o|$. [b] $R_w = (\sum(w|F_o| - |F_c|)^2)^{1/2}/(\sum wF_o^2)^{1/2}$; $w = (\sigma^2(F_o) + 0.0068F_o^2)^{-1}$.

Cu type, exhibits a ground state of low-spin multiplicity. The unexpected cancellation of the spins has tentatively been ascribed to the presence of nn exchange of positive sign along one chain and negative sign along the other chain. An approximate 2-D model yielded J values of $+0.56$ and -0.12 cm^{-1} for the two chains. However, the lack of confirmatory experimental evidence for the presence of a 2-D magnetic lattice did not allow a reliable correlation between coupling constants and exchange pathways.

In this paper, we describe a new compound, $Cu(op)_2MnCl_4$ (op = 1,4-diazacycloheptane, $H_2N(CH_2)_5NH_2$), that is related to the en analogue in showing closely similar ligand bridges between the magnetic centers but differs from it in being comprised of chloride-bridged binuclear units. Variable-temperature magnetic susceptibility and single-crystal EPR data show that $Cu(op)_2MnCl_4$, owing to the Cu—N—H···Cl—Mn interdimer contacts, actually behaves as a pseudo-2-D magnetic system and that the dimers are ferromagnetically coupled. This novel result is explicable in terms of the local symmetries of the magnetic ions.

Experimental Section

Synthesis. A 0.85-g (5.0 mmol) quantity of $CuCl_2·2H_2O$ was dissolved in methanol (15 mL). The solution was added to a solution of the op ligand (1.00 g, 10.0 mmol) in the same solvent (20 mL). The addition was made over a period of 10 min, at 0 °C and with constant stirring. To the resulting blue solution was added dropwise 1.00 g (8.0 mmol) of $MnCl_2$ dissolved in 20 mL of ethanol. The reaction mixture was stirred for 2 h at 0 °C and then allowed to stand at room temperature for an additional 6 h. Red-violet, crystalline $Cu(op)_2MnCl_4$ was collected by filtration, washed with 1:1 ethanol—diethyl ether, and dried under vacuum: yield 0.84 g (34% based on original copper); mp 230—232 °C. Anal. Calcd for $C_{10}H_{24}N_4Cl_4CuMn$: C, 26.08; H, 5.25; N, 12.16. Found: C, 26.32; H, 5.30; N, 12.05.

Magnetic Measurements. Variable-temperature magnetic susceptibility and EPR experiments were performed in the range 4—290 K. Susceptibilities were measured in a magnetic field of 0.7 T with use of a Faraday type magnetometer equipped with a helium continuous-flow cryostat built by Oxford Instruments. Susceptibilities were corrected[10] for the diamagnetism of the ligand system (-260×10^{-6} emu·mol^{-1}) and for the temperature-independent paramagnetism, Nα, of copper(II) (estimated to be 60×10^{-6} emu/Cu atom).

Polycrystalline powder and single-crystal EPR spectra were recorded with a Varian E-9 spectrometer equipped with standard X-band facilities and with an Oxford Instruments ESR 9, continuous-flow cryostat.

Crystallographic Data Collection and Structure Determination. A red-violet prismatic crystal with dimensions $0.20 \times 0.15 \times 0.12$ mm^3 was mounted on a computer-controlled Philips PW1100 single-crystal diffractometer equipped with a graphite-monochromatized Mo Kα radiation. Cell parameters were determined by a least-squares calculation based on the setting angles of 30 reflections with 2θ angles ranging from 16 to 25°. Cell dimensions and additional crystal data are listed in Table 1. The space group resulted from systematic extinctions. The intensities of the $\pm hkl$ reflections were collected up to $2\theta = 50°$. The $\omega-2\theta$ scan technique was employed, the scan range being 1.8° and the speed 0.06 deg s^{-1}. A total of 2330 independent reflections was measured: of these, 889, having $I \leq 3\sigma(I)$, were considered as "unobserved" and excluded from the refinement. Three standard reflections monitored every 100 min showed no apparent variation in intensity during the data collection. The data were corrected for Lorentz—polarization factors. No absorption correction was applied.

The structure was solved by direct methods using the SIR88 program[11] and refined by the full-matrix least-squares method with use of the SHELX-76 package of programs.[12] Anisotropic thermal parameters were refined only for the heavier atoms, Cu, Mn, and Cl. The atomic scattering factors were taken from ref 12 for the Cl, C, and N atoms and from ref 13 for the Cu and Mn atoms: a correction for anomalous dispersion was included. The refinement was carried out with 112 parameters and 1441 oserved reflections. The final unweighted R factor was 0.059 ($R_w = 0.062$). This rather high value can be ascribed to the presence of twinning, as indicated by some very weak reflections with Miller indices violating the extinction rules of the space group. In an attempt at finding an untwinned sample, several other crystals from different crystallization batches were tested and new intensity data collected, but the results of the refinements with these different data sets did not improve. In spite of these shortcomings, the obtained structural information can be considered suitable for our purposes. Final positional parameters are given in Table 2.

Table 2. Positional Parameters ($\times 10^4$) and Equivalent Isotropic Displacement Coefficients (Å$^2 \times 10^3$) for $Cu(op)_2MnCl_4$

	x/a	y/b	z/c	$U_{eq}{}^a$
Cu	2750(1)	6018(1)	3605(2)	28(1)
Mn	2968(1)	3796(1)	8159(3)	31(1)
Cl(1)	3281(2)	5035(2)	6740(5)	47(2)
Cl(2)	3583(2)	3881(2)	11431(5)	48(2)
Cl(3)	3401(2)	2550(2)	7036(5)	51(2)
Cl(4)	1414(2)	3700(2)	7822(5)	48(2)
N(1)	1551(6)	6285(5)	4222(14)	32(2)
N(2)	1989(5)	5174(4)	2094(13)	26(2)
N(3)	3414(6)	7039(5)	4453(15)	41(2)
N(4)	3905(6)	5815(6)	2711(15)	46(3)
C(1)	1123(8)	5500(7)	4674(18)	44(3)
C(2)	1399(7)	4825(7)	3307(18)	40(3)
C(3)	1463(7)	5594(7)	395(17)	37(3)
C(4)	749(8)	6126(7)	976(19)	44(3)
C(5)	1028(7)	6712(7)	2578(18)	38(3)
C(6)	4329(7)	6802(8)	5347(18)	45(3)
C(7)	4635(8)	6039(7)	4334(19)	47(3)
C(8)	3945(10)	6338(9)	992(23)	62(4)
C(9)	4034(9)	7221(9)	1432(23)	66(4)
C(10)	3428(8)	7548(8)	2706(18)	47(3)

[a] The equivalent isotropic U for anisotropically refined atoms is defined as one-third of the trace of the $\mathbf{U}_{ij}$ tensor.

Results

Description of the Structure. The structure of the compound consists of chloride-bridged $Cu(op)_2MnCl_4$ binuclear units. The molecule and labeling scheme are shown in Figure 1.

The Mn(II) coordination environment is distorted-tetrahedral. The main deviation from tetrahedral symmetry is represented by the Cl(1)—Mn—Cl(3) bond angle of 121.7(1)°. The Cu(II) ion has (4 + 1) square-pyramidal geometry. The four short bonds are to the nitrogens of the organic ligands, and the long, apical bond involves the bridging Cl(1) ion.

The bridging Cu—Cl(1) bond distance is 2.775(3) Å and the Cu—Cl(1)—Mn bridging angle is 143.2(1)°. The intradimer Cu···Mn separation is 4.892 Å.

(10) Mabbs, F. E.; Machin, D. J. *Magnetism and Transition-Metal Compounds*; Chapman and Hall: London, 1973.

(11) Burla, M. C.; Camalli, M.; Cascarano, G.; Giacovazzo, C.; Polidori, G.; Spagna, R.; Viterbo, D. *J. Appl. Crystallogr.* **1989**, *22*, 389.

(12) Sheldrick, G. M. *SHELX-76*, Program for Crystal Structure Determination; University of Cambridge: Cambridge, U.K., 1976.

(13) *International Tables for X-ray Crystallography*; Kynoch Press: Birmingham, U.K., 1974; Vol. IV, p 99.

Table 3. Selected Bond Lengths (Å) and Angles (deg)

Cu−N	2.011(9)	Mn−Cl(1)	2.379(3)
Cu−N(2)	2.012(8)	Mn−Cl(2)	2.367(4)
Cu−N(3)	2.017(9)	Mn−Cl(3)	2.355(3)
Cu−N(4)	2.012(10)	Mn−Cl(4)	2.356(3)
Cu−Cl(1)	2.775(3)		
N(1)−Cu−N(2)	78.8(3)	N(4)−Cu−Cl(1)	90.4(3)
N(2)−Cu−N(3)	164.1(4)	Cl(1)−Mn−Cl(2)	107.1(1)
N(3)−Cu−N(4)	79.1(4)	Cl(1)−Mn−Cl(3)	121.7(1)
N(4)−Cu−N(1)	173.6(4)	Cl(1)−Mn−Cl(4)	106.8(1)
N(4)−Cu−N(2)	99.9(4)	Cl(2)−Mn−Cl(3)	107.5(1)
N(3)−Cu−N(1)	100.5(4)	Cl(2)−Mn−Cl(4)	109.0(1)
N(1)−Cu−Cl(1)	95.9(3)	Cl(3)−Mn−Cl(4)	104.2(1)
N(2)−Cu−Cl(1)	94.9(2)	Cu−Cl(1)−Mn	143.2(1)
N(3)−Cu−Cl(1)	101.0(3)		

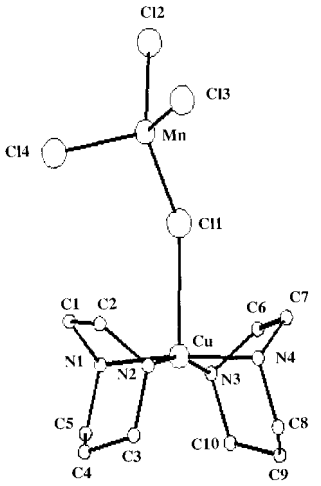

Figure 1. View of the $Cu(op)_2MnCl_4$ unit.

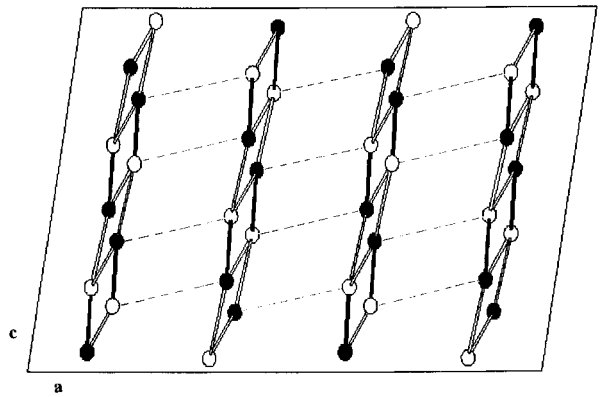

Figure 2. Schematic representation of the layer structure of $Cu(op)_2MnCl_4$. The empty and filled circles represent the Mn and Cu atoms, respectively. The thick segments indicates the Mn−Cl−Cu bridges, the double lines the Mn−Cl···H−N−Cu bridges, and the dashed lines the shortest M···M contacts between layers.

In the crystal, the binuclear units assemble in layers parallel to (1 0 0). As indicated in Figure 2, the shortest M···M contact between layers, 6.897 Å, occurs between Mn and the Cu atom at $1 - x$, $1 - y$, $1 - z$. Also, no close contacts among atoms involved in the magnetic orbitals occur between adjacent layers. The closest N···Cl contacts are longer than 4.5 Å.

The arrangement of the binuclear units within a layer is schematically shown in Figure 3.

The shortest M···M and N···Cl separations between nearest neighboring dimers are $Mn\cdots Cu^{I} = 5.359$ Å ($^{I} = {}^{1}/_{2} - x, -{}^{1}/_{2} + y, {}^{3}/_{2} - z$), $Cu\cdots Mn^{II} = 5.413$ Å ($^{II} = x, y, z + 1$), $Cl(3)\cdots N(1)^{I} = 3.390$ Å, $Cl(4)\cdots N(3)^{I} = 3.360$ Å, $Cl(2)\cdots N(2)^{II} = 3.346$ Å, and $Cl(2)\cdots N(4)^{II} = 3.352$ Å.

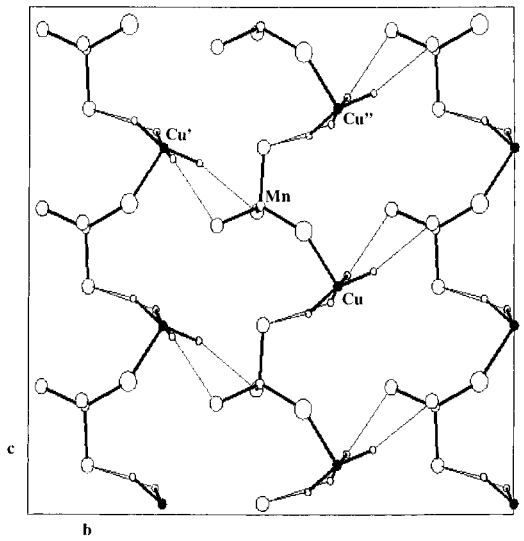

Figure 3. Arrangement of the binuclear units within a layer. The thin lines indicate the N···Cl contacts discussed in the text.

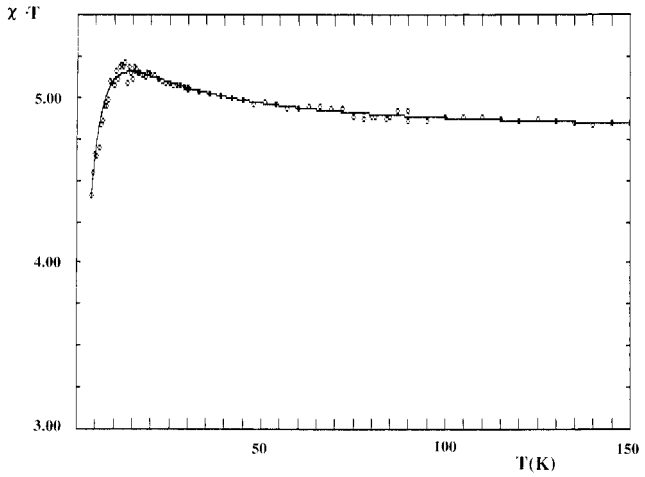

Figure 4. Experimental and theoretical temperature dependence of χT for $Cu(op)_2MnCl_4$ between ca. 4 and 150 K. The solid line through the data was generated by the mean field corrected dimer model illustrated in the text.

The interdimer N···Cl distances are not significantly different from the sum of van der Waals radii[14] of N and Cl, 3.30 ± 0.10 Å, so, as in the case[5] of $Cu(en)_2MnCl_4$, there is no structural evidence for the presence (or absence) of attractive hydrogen-bonding interactions.

Magnetic Properties. The temperature dependence of the magnetic susceptibility for $Cu(op)_2MnCl_4$ is shown in Figure 4, in the form of the χT vs T plot, χ being the corrected molar magnetic susceptibility per MnCu unit. At room temperature, χT has a value of 4.84 emu·mol^{-1}·K, slightly larger than that expected for uncoupled $S = {}^{5}/_{2}$ and $S = {}^{1}/_{2}$ spins (4.75 emu·mol^{-1}·K for $g_{Mn} = g_{Cu} = 2$). When the temperature is lowered, χT remains almost constant until 80−90 K, increases to reach a maximum at ~13 K (5.21 emu·mol^{-1}·K), and then rapidly decreases.

The room-temperature EPR spectrum of polycrystalline powdered samples of the compound shows an isotropic signal at $g = 2.023$, with a peak-to-peak line width of 195 G. Below ~80 K, the spectrum becomes more and more anisotropic without showing significant variations in line width. A single-crystal study was undertaken in order to better resolve the

(14) Pauling, L. *The Nature of the Chemical Bond*, 3rd ed.; Cornell University Press: Ithaca, NY, 1960.

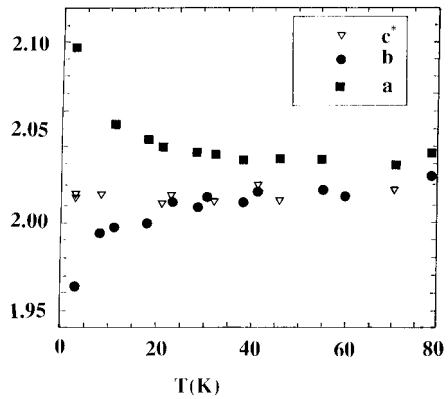

Figure 5. Temperature dependence of the g values of $Cu(op)_2MnCl_4$ observed at three different settings of the magnetic field.

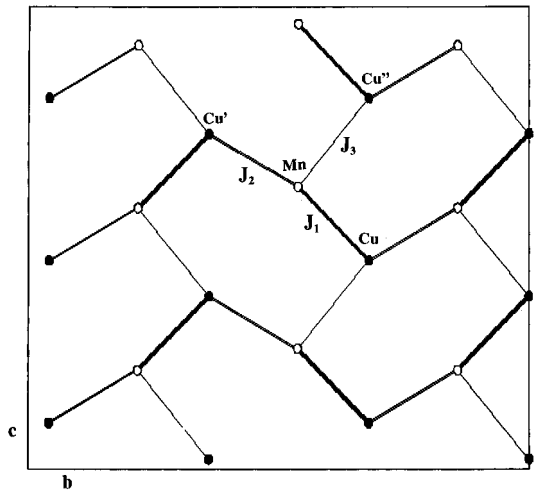

Figure 6. Sketch of the 2-D network of exchange interactions in $Cu(op)_2MnCl_4$.

anisotropy in the resonant fields. Spectra were recorded on crystals rotated around the *a*, *b*, and *c** orthogonal axes. A Lorentz line shape was observed for every crystal orientation. The temperature dependence of the *g*-factors of the broad EPR absorption in the low-temperature region is shown in Figure 5, where it can be seen that particularly large *g*-shifts occur below ~20 K. The largest shift is positive and is observed along the *a* direction: g_a increases up to about 2.10 at 4.2 K. At the same temperature the resonance parallel to *b* is observed at $g = 1.96$, and that parallel to *c**, at $g = 2.01$. The sum of the *g*-shifts is very close to zero.

Discussion

The structure of the compound consists of magnetically isolated layers. As shown in Figure 3, three nn exchange interactions, corresponding to three different Mn···Cu separations, potentially occur in a layer: one within the clusters, J_1, and the other two, J_2 and J_3, between clusters. The 2-D network of interactions generated by these couplings is sketched in Figure 6.

Exchange J_1 occurs through the Mn—Cl—Cu pathway, corresponds to a Mn···Cu separation of 4.892 Å, and involves out-of-plane unpaired electron density of square-pyramidal copper(II). By contrast, the J_2 and J_3 exchanges involve Mn—Cl···H—N—Cu pathways, considerably longer Mn···Cu distances (5.359 and 5.413 Å, respectively), and Cu(II) in-plane unpaired electron density. These features suggest $J_1 \neq J_2 \sim J_3$.

The magnetic susceptibility data are in agreement with the presence of two types of interactions in showing a gradual rise in χT as T initially decreases below 80−90 K and a precipitous drop in χT at low temperature. A rigorous estimate of J_1, J_2, and J_3 involves the solution of a 2-D Hamiltonian with three coupling constants between alternating $S = {}^5/_2$ and $S = {}^1/_2$ spins. Such a Hamiltonian, owing to its complexity, cannot presently be used for data analysis unless drastic approximations are made.

The simplest one is to assume that the strongest coupling constant correspond to the shortest Mn···Cu separation and that, in addition, the small differences between the interdimer J_2 and J_3 paths may be neglected. With $|J_1| \gg |J_2| = |J_3|$, the susceptibility can be approximated by using a mean field corrected[15,16] dimer model with an interaction J_1 within the dimer and J_2 between dimers. The susceptibility equation (per Mn—Cu pair, and writing the exchange constant as $-2J$) has the form (1), where z is the number of nearest neighbors of the dimers (4 in this case), χ_{dimer} is given by eq 2 and other symbols have their usual meaning.

$$\chi = \chi_{dimer}/[1 - \chi_{dimer}(2zJ_2/Ng^2\mu_B{}^2)] \quad (1)$$

$$\chi_{dimer} = (N\mu_B{}^2/kT)[10g_2{}^2 + 28g_3{}^2 \exp(6J_1/kT)]/[5 + 7\exp(6J_1/kT)] \quad (2)$$

$$g_2, (S = 2) = (7g_{Mn} - g_{Cu})/6;$$

$$g_3, (S = 3) = (5g_{Mn} + g_{Cu})/6$$

The best fit of eq 1 to the data was achieved with $J_1 = 2.58(1)$ cm^{-1} and $J_2 = -0.07(1)$ cm^{-1} (which satisfy the requirement $|J_1| \gg |J_2|$), $g_2 = 1.99(1)$, and $g_3 = 2.01(1)$. The agreement factor, defined as $F = \sum(\chi_i{}^{obs})^{-1}(\chi_i{}^{obs} - \chi_i{}^{calc})^2$, was $F = 1.8 \times 10^{-3}$, for 80 observations. As in subsequent calculations, only data below 150 K were used. As it also appears from Figure 4, the fit may be considered as fairly good. The ratio between interdimer and intradimer exchange is $4|J_2/J_1| = 0.1$ and suggests a pseudo-2-D magnetic structure.

Exchange was also estimated with use of a slight modification of a previously proposed model[5,17] which mimicks a 2-D system as a chain of chains. The dimeric unit is assumed to act as an effective S_d classical spin system (whatever the temperature may be, $2 \leq S_d \leq 3$) so that the magnetic lattice consists of cross-linked, uniformly-spaced chains (directed along *b* and *c*, respectively) of interacting S_d spins. To generate the susceptibility, we first obtain the effective S_d spin as

$$S_d = \{-1 + [1 + 4\chi_d T/(0.1251g_d{}^2)]^{1/2}\}/2 \quad (3)$$

where χ_d is given by eq 2. Then we consider a J_b interaction between nn S_d spins along the *b* (or *c*) directed chain. The susceptibility of such a chain, χ_b is given by eq 4. Finally we

$$\chi_b = [N\mu_B{}^2 g_d{}^2 S_d(S_d + 1)/3kT](1 + \mu)/(1 - \mu) \quad (4)$$

$$\mu = \coth(K) - 1/K; \quad K = 2J_bS_d(S_d + 1)/kT$$

use χ_b to obtain the effective S_b spin for the MnCu pair in the *b* chain using eq 5 and calculate the susceptibility of the 2-D system as that, eq 6, of a *c* directed chain of S_b spins coupled

(15) Myers, B. E.; Berger, L.; Friedberg, S. A. *J. Appl. Phys.* **1968**, *40*, 1149.
(16) Smart, J. S. *Effective Field Theories of Magnetism*; Saunders: Philadelphia, PA, 1966.
(17) Caneschi, A.; Gatteschi, D.; Melandri, M. C.; Rey, P.; Sessoli, R. *Inorg. Chem.* **1990**, *29*, 4228.

by a J_c exchange constant. Assuming $g_d = g_b = g_c = 2.023$,

$$S_b = \{-1 + [1 + 4\chi_b T/(0.1251 g_b^2)]^{1/2}\}/2 \quad (5)$$

$$\chi_c = [N\mu_B^2 g_c^2 S_b(S_b + 1)/3kT)](1 + u)/(1 - u) \quad (6)$$

$$\mu = \coth(P) - 1/P; \quad P = 2J_c S_b(S_b+1)/kT$$

the experimentally determined EPR $\langle g \rangle$ value, an accurate best fit ($F = 7.8 \times 10^{-4}$) of eq 6 to the data was achieved with $J_1 = 2.68(1)$ cm^{-1}, $J_b = -0.04(1)$ cm^{-1}, $J_c = -0.03(1)$ cm^{-1}, $g_2 = 1.99(1)$, and $g_3 = 2.01(1)$. The parameters are in agreement with the results obtained with the previous model, and the calculated χT vs T curve is virtually superimposable on that shown in Figure 4.

To sum up, the fitting calculations attribute the rise in χT as T initially decreases below 80−90 K to a state where the $^5/_2$ and $^1/_2$ spins tend to be parallel within uncorrelated dimers and the drop in χT below ∼13 K to a state where short-range antiferromagnetic coupling among neighboring dimers leads to cancellation of the spins. An alternative explanation of the χT drop in terms of selective thermal population of zero-field splitting levels within the dimer septet ground state (the quintet is $6J$ in energy above it) does not appear to be relevant here. The energy separation between the highest and lowest level within the septet state at zero field is $9|D|$, where D is the conventional axial zero-field splitting parameter.[18] The $\mathbf{D}_3$ tensor for the $S = 3$ state is related to $\mathbf{D}_{Mn}$ through $\mathbf{D}_3 = 2\mathbf{D}_{Mn}/3$.[19] In a distorted tetrahedral crystal field $\mathbf{D}_{Mn}$ is typically of the order of 10^{-2} cm^{-1}.[18−20] Then, in light of the present relatively high Mn(II) site symmetry, it can safely be assumed that $kT \gg 9|D|$, between 13 and 4.2 K. Likewise, the rapid decrease of the χT curve below 13 K cannot be accounted for by the saturation effects of the magnetic field.[21]

More important, the intermolecular, 2-D picture is fully substantiated by the single-crystal EPR data for the compound. The spectra show an effective g-value which, although isotropic at high temperatures, becomes increasingly anisotropic at low temperatures. Such behavior is typical of low-dimensional magnetic systems, most likely arising from short-range correlation effects.[19,22−27] It has recently been suggested[28] that increasing g-anisotropy at low temperatures might also be due to demagnetizing fields. The fact that the present shifts are observed even in the polycrystalline powder spectra and calculation of the demagnetizing fields for our crystal suggest that this contribution can at best account for a small fraction of the observed shifts. Also, relevant zero-field splitting effects on the observed g anisotropy are not conceivable here: the presence of zero-field splitting does not cause g anisotropy unless $D \gg h\nu_0$ and in such a case it is expected to give $g_{\|} = 2$ and $g_{\perp} = 4$ or 6.[19]

In general, the resonance field of a low-dimensional magnetic material is isotropic at high temperatures because kT is much larger than the exchange energy, so that the relative spin orientations are completely random. At low enough temperatures, however, kT no longer overwhelms the exchange energy and short-range correlations may occur among the spins. The EPR resonance fields, and the susceptibility likewise, become anisotropic because the short-range ordered spins have a preferred orientation in the lattice which enables the corresponding local fields to oppose or augment the applied static field.

For a Mn(II)···Cu(II) system, the preferred spin orientation is most likely determined by dipolar interactions.[18,26,27,29] Accordingly, in the 2-D case, the lowest energy arrangement is within the plane when the spins are parallel to each other and perpendicular to the plane when the spins are antiparallel. The resonance fields along the three principal axes can be expressed[30−32] as in eq 7, where χ_a, χ_b and χ_c are the principal

$$B_a = [(\chi_b\chi_c)^{1/2}/\chi_a]B_0 \quad (7)$$

susceptibilities in the paramagnetic region and B_0 is the resonance field in the absence of short-range order (the resonance fields along the b and c crystal directions follow from cyclic permutations).

For the present system the resonance fields are found to shift upfield (producing a negative g-shift) parallel to the plane and downfield (positive g-shift) perpendicular to the plane. With the aid of Figure 6 and eq 7, it can be seen that this may occur either because the inequivalent $^5/_2$ and $^1/_2$ spins are oriented perpendicular to the plane, owing to a dominant nn antiferromagnetic coupling, or because spin cancellation takes place between spins oriented within the plane. The former possibility is not tenable since it would imply an overall ferrimagnetic arrangement, and, in the limit of T approaching zero, $\chi_{av}T$ should diverge instead of tending to zero as observed. On the other hand, in order to have in-plane spin cancellation, it is necessary that the strongest of the J_1, J_2, and J_3 coupling constants is ferromagnetic, so as to keep the spins within the plane, and the other two, of weaker magnitude, antiferromagnetic. In light of the already mentioned similarity of the J_2 and J_3 exchange pathways and the fitting results for the magnetic susceptibility it is reasonably concluded that $J_1 > 0$ and J_2, $J_3 < 0$.

The quite unusual Mn(II)···Cu(II) exchange coupling of opposite sign in $Cu(op)_2MnCl_4$ (and, by inference, in the related $Cu(en)_2MnCl_4$ compound) is explicable in terms of the commonly accepted notion that overlap of the magnetic orbitals favors antiferromagnetic coupling, whereas orthogonality leads to ferromagnetic coupling.[33−35]

The $MnCl_4$ fragment approximates tetrahedral symmetry, so the five magnetic orbitals centered on Mn(II) have delocalization tails on the p′ orbitals of each chlorine atom. Copper is instead in a square-pyramidal CuN_4Cl environment with the bridging Cl atom occupying the apical position. As the site symmetry

(18) Carlin, R. L. *Magnetochemistry*; Springer-Verlag: Berlin, 1986.
(19) Bencini, A.; Gatteschi, D. *EPR of Exchange Coupled Systems*; Springer-Verlag: Berlin, 1990.
(20) McGarvey, B. R. In *Transition Metal Chemistry*; Carlin, R. L., Ed.; Dekker: New York, 1966; Vol. 3, p 170.
(21) Caneschi, A.; Ferraro, F.; Gatteschi, D.; Rey, P.; Sessoli, R. *Inorg. Chem.* **1990**, *29*, 4217.
(22) Gatteschi, D.; Sessoli, R. *Magn. Reson. Rev.* **1990**, *15*, 1.
(23) Tanake, K.; Tazuke, Y. *J. Phys. Soc. Jpn.* **1972**, *32*, 337.
(24) Oshima, K.; Okuda, K.; Date, M. *J. Phys. Soc. Jpn.* **1977**, *43*, 1131.
(25) Caneschi, A.; Gatteschi, D.; Sessoli, R.; Cabello, C. I.; Rey, P.; Barra, A. L.; Brunel, L. C. *Inorg. Chem.* **1991**, *30*, 1882.
(26) Caneschi, A.; Gatteschi. D.; Renard J.-P.; Rey, P.; Sessoli, R. *Inorg. Chem.* **1989**, *28*, 1976.
(27) Gatteschi, D.; Guillou, O.; Zanchini, C.; Sessoli, R.; Kahn, O.; Verdaguer, M.; Pei, Y. *Inorg. Chem.* **1989**, *28*, 297.
(28) Oshima, K.; Kawanone, H.; Haybara, Y.; Yamazaki, I.; Awaga, K.; Tamura, M.; Kinoshita, M. *Proceedings of International Conference on Synthetic Metals*, Seoul, 1994. Cirujeda, J.; Hernandez-Gaziò, E.; Rovira, C.; Sranger, J. L.; Turek. P.; Veciana, J. *J. Mater. Chem.* **1995**, *5*, 243.
(29) Kahn, O.; Pei, Y.; Verdaguer, M.; Renard, J.-P.; Sletten, J. *J. Am. Chem. Soc.* **1988**, *110*, 782.
(30) Karasudani, T.; Okamoto, H. *Phys. Lett.* **1976**, *57A*, 77.
(31) Karasudani, T.; Okamoto, H. *J. Phys. Soc. Jpn.* **1977**, *43*, 1131.
(32) Okamoto, H.; Karasudani, T. *J. Phys. Soc. Jpn.* **1977**, *42*, 717.
(33) Hay, P. J.; Thibeault, J. C.; Hoffmann, R. J. *J. Am. Chem. Soc.* **1975**, *97*, 4884.
(34) Kahn, O. *Molecular Magnetism*; VCH: Weinheim, Germany, 1993.
(35) Cotton, F. A. *Chemical Applications of Group Theory*, 3rd ed.; Wiley: New York, 1990. Ballhausen, C. J. *Ligand Field Theory*; McGraw-Hill: New York, 1962.

at Cu(II) is very nearly C_{2v}, the metal unpaired electron is described by an *xy*-like orbital transforming as a_2 and delocalized on the nitrogen ligands only. The magnetic orbital cannot contain contributions from out-of-plane metal d orbitals since, in C_{2v}, z^2 transforms as a_1 and *xz* and *yz* as b_1 and b_2, respectively.

On this basis, the negative sign of the interdimer J_2 and J_3 exchanges, that are mediated by the Cu—N—H···Cl—Mn pathways, can be ascribed to the overlap, albeit very weak, between the delocalization tails of the Cu(II) and Mn(II) open shells.

As for the exchange propagated by the Cu—Cl—Mn pathway, J_1, the relative orientation of the *xy* orbital of Cu(II) and the p′ orbitals on the Cl bridge (the delocalization tails of the Mn(II) magnetic orbitals) is depicted as follows (vectors represent the positive orbital lobes), where the conventional tetrahedral coordinate system[35] is used for the p′ orbitals on Cl and the molecular *z* axis is collinear with Cu—Cl.

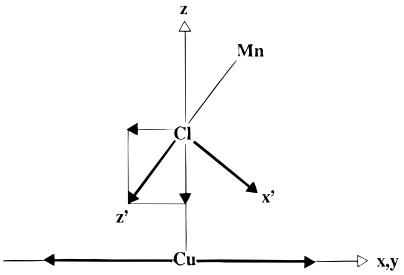

The positive sign of J_1 can be traced back to the orthogonality between the *xy*-like magnetic orbital on Cu(II) and the p′ orbitals on the bridging Cl atom. Indeed, in whatever way the p′ orbitals may be inclined to the Cu—Cl axis, the overlap integral $S[(xy)_{Cu},(p_i')_{Cl}]$, where $i = x'$, y', or z', evaluates to zero. This can simply be realized by resolving the p′ functions of Cl in the coordinate frame used for the Cu(II) magnetic orbital and noting that the component p_x, p_y, and p_z orbitals in the new set of axes are orthogonal to the *xy* orbital of Cu(II) because of the different symmetry about the *z* (Cu—Cl) axis. Similar arguments can be used to explain the ferromagnetic coupling propagated by one Cu—SCN—Mn exchange pathway in $\{[Cu(en)_2]_3[Mn(NCS)_6]\}(NCS)_2$.[9]

A last comment concerns the relative strength of the ferromagnetic interactions in the op ($\sim$2.6 cm^{-1}) derivative and the en analogue ($\sim$0.6 cm^{-1}).

Basically, the $Cu(op)_2MnCl_4$ dimer, neglecting the C_{2v} distortion in its $MnCl_4$ fragment, may be generated from the $Cu(en)_2MnCl_4$ binuclear unit by increasing the Cu—Cl—Mn bridging angle from 124.6° to 143.2°, rotating the $MnCl_4$ tetrahedron around the Cl(bridge)—Mn axis by 41.9°, and shortening the Cl(bridge)—Cu distance, R_0, by 0.16 Å. Simple calculations show that, for a given R_0, the rotations lead to a larger π-type p(Cl)/*xy*(Cu) overlap density leaving the axial one almost unchanged. In light of this,[4] and, more importantly, because both axial and π overlap densities are expected to increase rapidly as R_0 decreases, a stronger ferromagnetic interaction for the op dimer might not be too surprising.

Acknowledgment. The financial support of the CNR, of the Progetto Finalizzato "Materiali Speciali per Tecnologie Avanzate", and of MURST is gratefully acnowledged.

Supporting Information Available: Tables giving bond lengths, bond angles, and anisotropic thermal parameters (2 pages). Ordering information is given on any current masthead page.

IC960373U